Supplementary Information

Structural features and their functions in surfactant-armoured methylammonium lead iodide perovskites for highly efficient and stable solar cells

Minsu Jung,[a] Tae Joo Shin,[b] Jangwon Seo,[c] Gwisu Kim[a] and Sang Il Seok*[a]

[a] School of Energy and Chemical Engineering, Ulsan National Institute of Science and Technology (UNIST), Ulsan 44919, South Korea

E-mail: seoksi@unist.ac.kr

[b] UNIST Central Research Facilities (UCRF), Ulsan National Institute of Science and Technology (UNIST), Ulsan 44919, South Korea

[c] Division of Advanced Materials, Korea Research Institute of Chemical Technology (KRICT), Deajeon 34114, South Korea

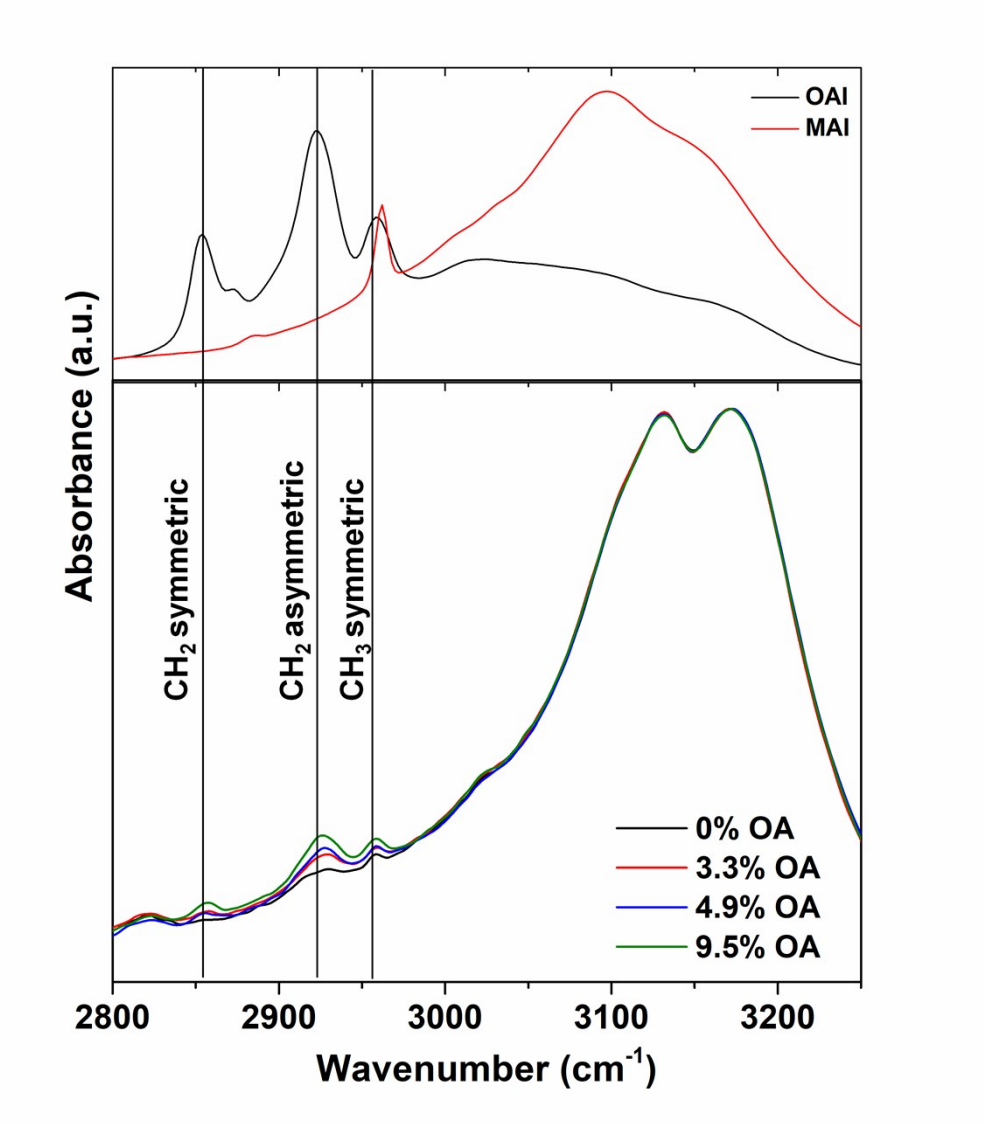

Fig. S1 Fourier transform infrared spectroscopy (FTIR) spectra for OA-modified $MAPbI_3$ powders with 0 and 9.5% contents. Upper graph shows FTIR spectra for octylammonium iodide (OAI) and methylammonium iodide (MAI) materials as a control.

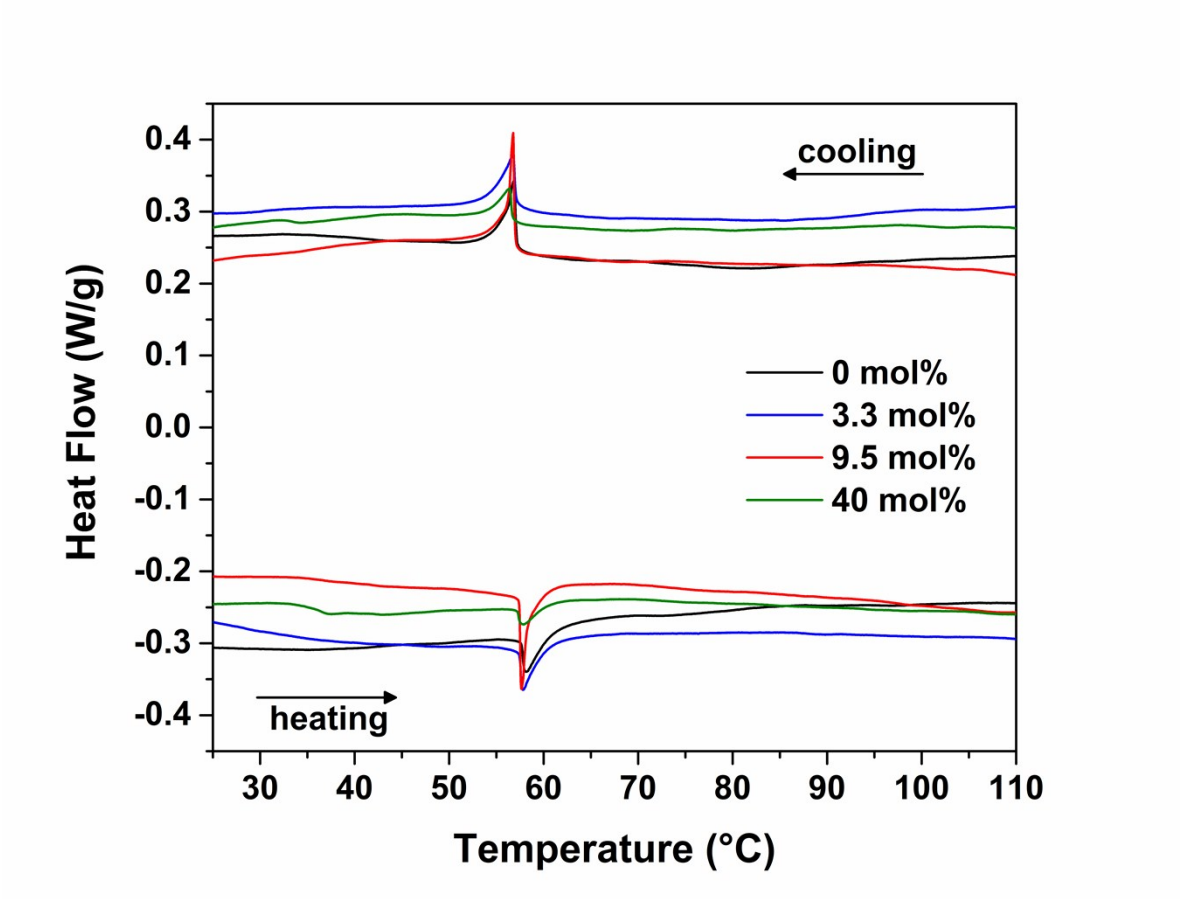

Fig. S2 Differential scanning calorimetry (DSC) curves for OA-modified perovskite powders with 0 and 9.5% contents. The DSC measurements were carried out at a temperature from 25 °C to 110 °C with a heating and cooling rate of 5 °C min^{-1} under nitrogen gas with a flow rate of 50 ml min^{-1}.

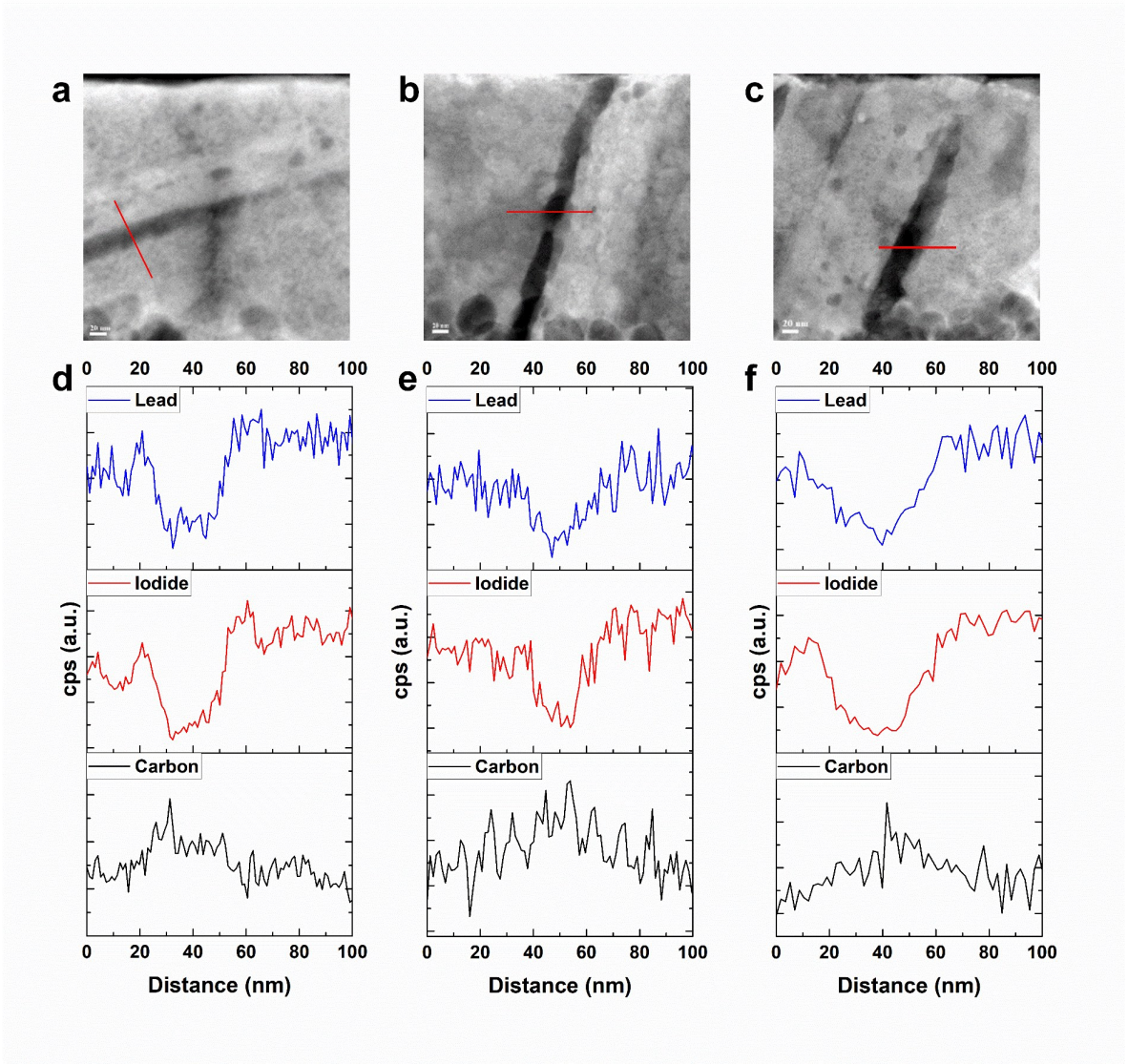

Fig. S3 Cross-sectional high-angle annular dark-field (HAADF)-scanning transmission electron microscopy (STEM) images of (a) 0%, (b) 3.3% and (c) 9.5% OA-modified $MAPbI_3$ films deposited on mp-TiO_2/bl-TiO_2/FTO. The length of scale bar in the STEM images is 20 nm. Red line in the images indicates the scanned positions for EDX elemental mapping. (d-f) Compositional profiles of lead, iodide and carbon through EDX mapping analysis by line scanning at GBs from (a-c).

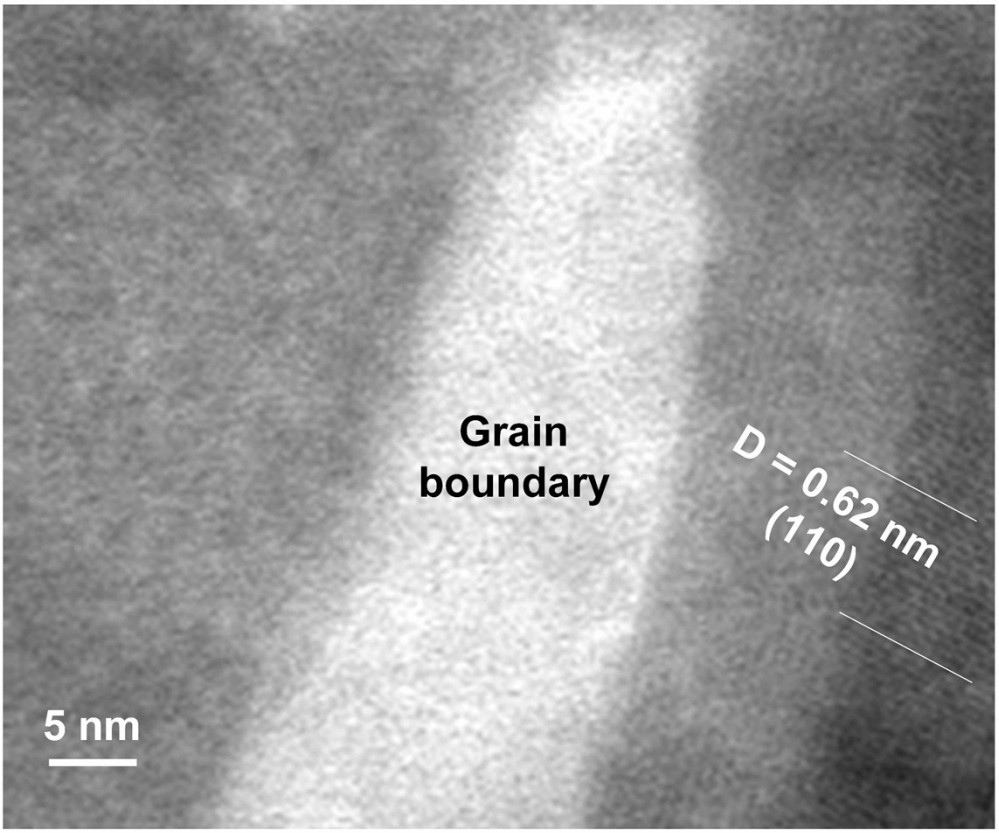

Fig. S4 Bright-field scanning transmission electron microscopy (STEM) cross-sectional image of 3.3 mol% OA-modified $MAPbI_3$ films deposited on mp-TiO_2/bl-TiO_2/FTO.

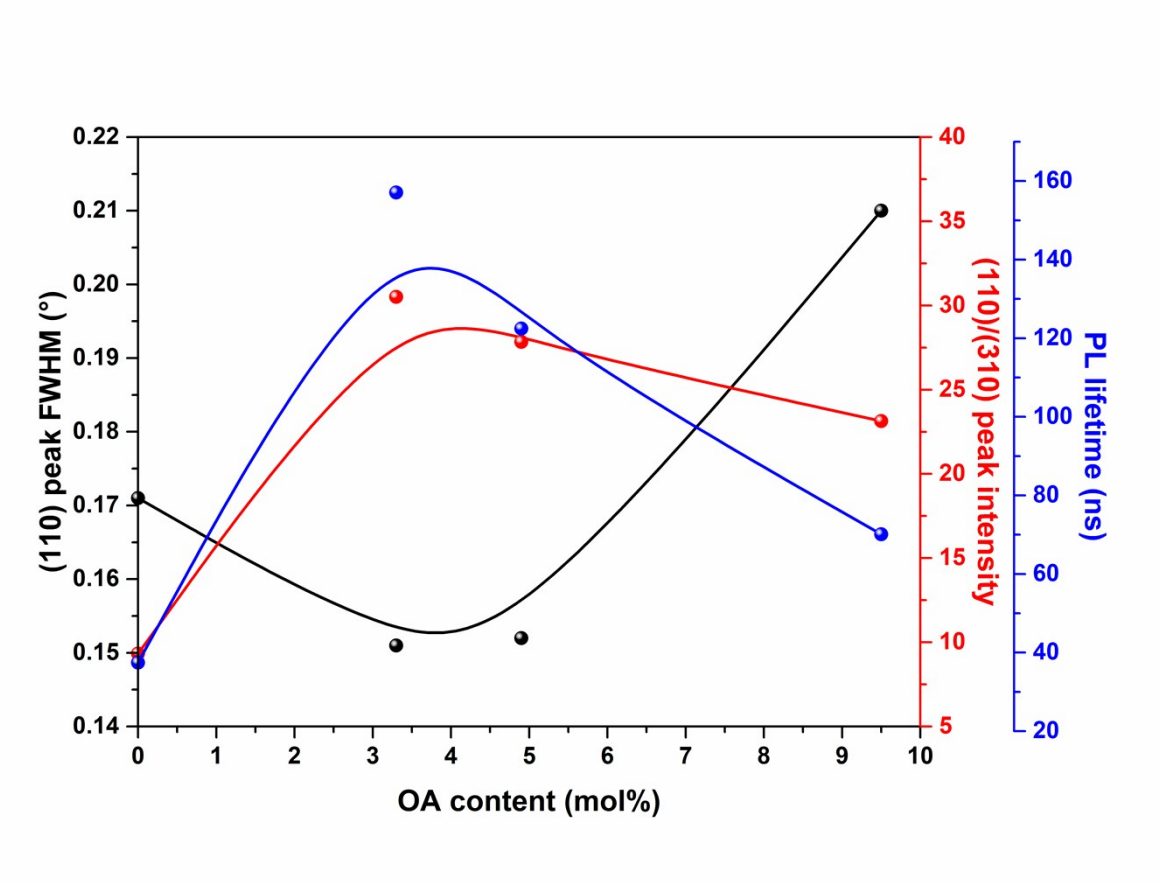

Fig. S5 Full width at half maximum (FWHM) of (110) peak, (110)/(310) peak intensity ratio from Fig. 1a, and time-resolved photoluminescence (TRPL) lifetimes calculated from Fig. 1c as a function of OA contents.

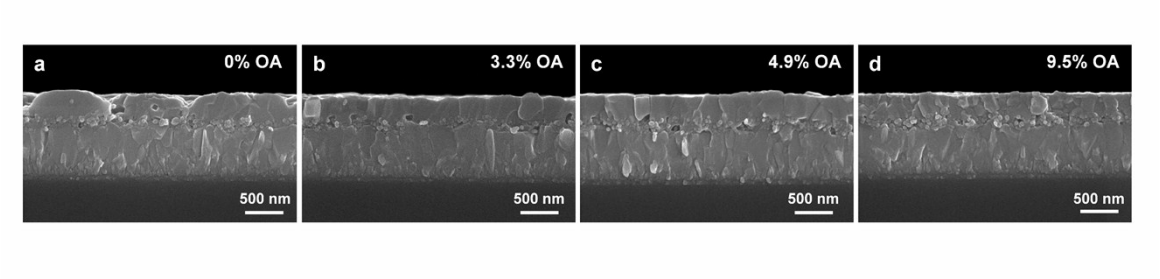

Fig. S6 (a-d) Cross-sectional scanning electron microscope (SEM) images of OA-modified perovskite films with 0 – 9.5% OA contents deposited on mp-TiO_2/bl-TiO_2/FTO.

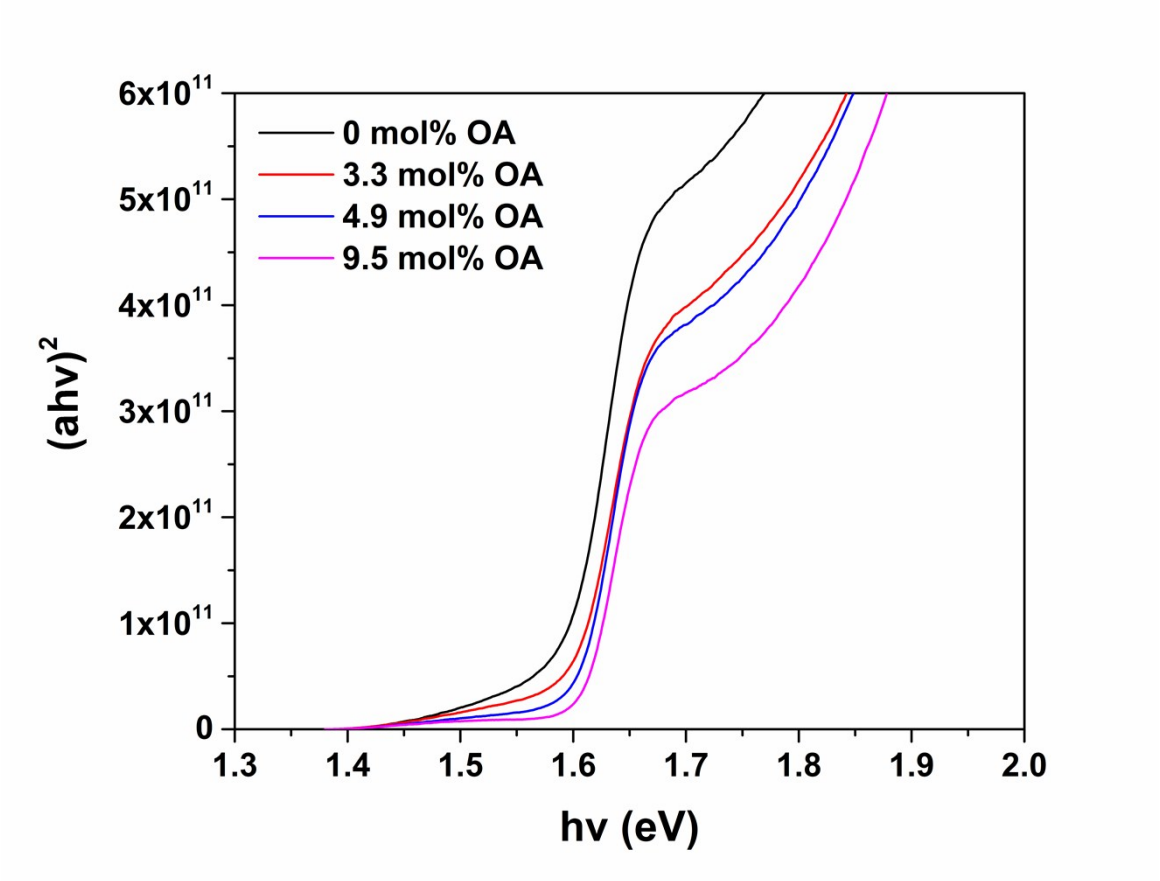

Fig. S7 Optical absorption spectra for perovskite films with OA contents ranging from 0 and 9.5%.

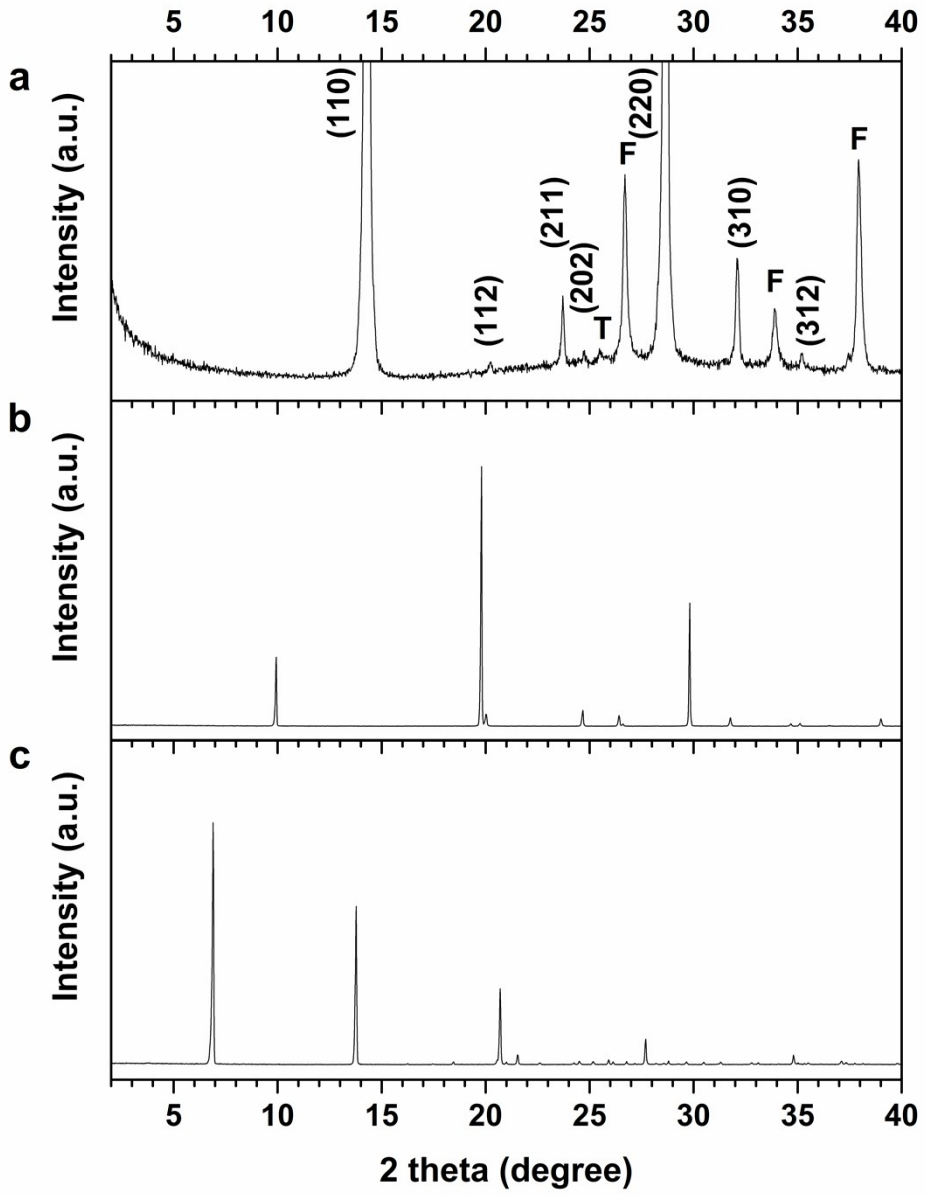

Fig. S8 XRD pattern magnified from Figure 1-(a) of (a) 3.3% OA-modified $MAPbI_3$. Diffraction peaks for FTO and anatase TiO_2 crystals are marked with F and T, respectively. (b) methylammonium iodide and (c) octylammonium iodide materials were used as a control.

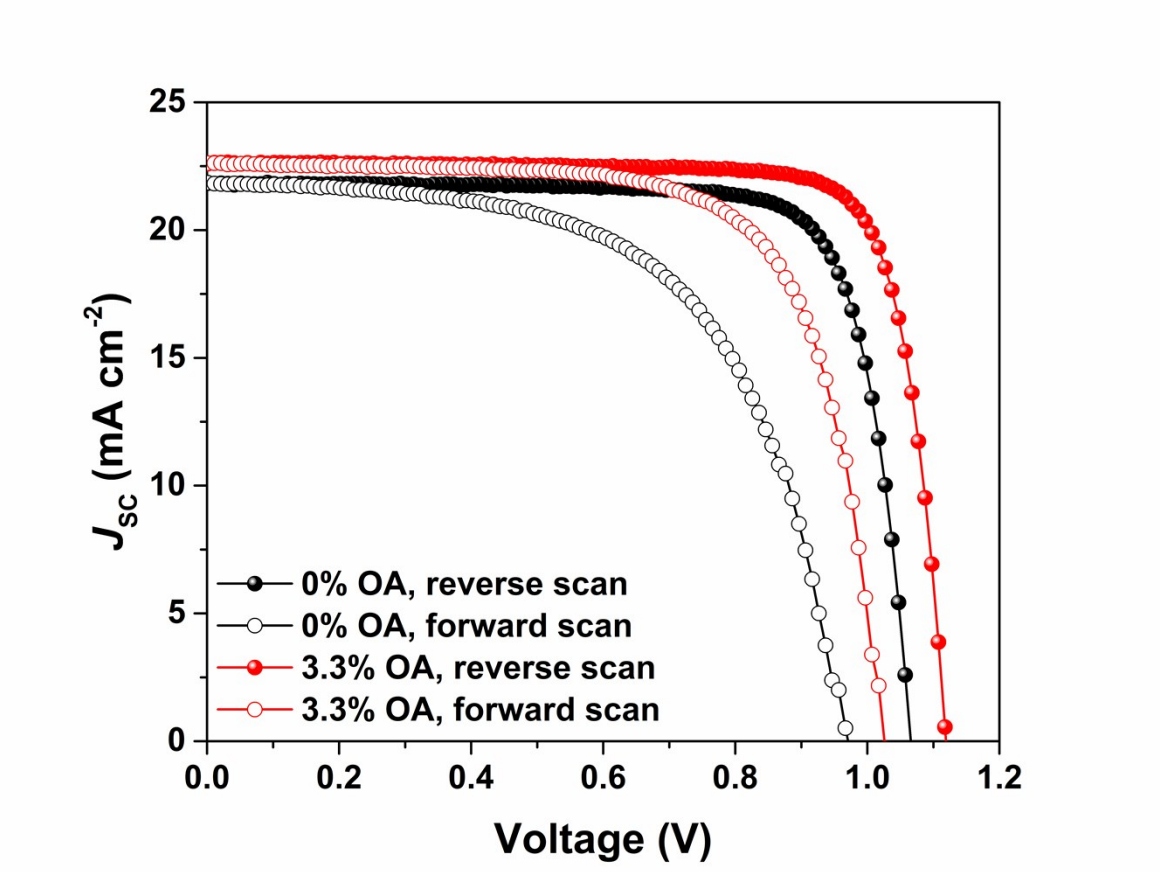

Fig. S9 *J-V* characteristics of 0% and 3.3% OA-modified perovskite films from reverse and forward scanning.

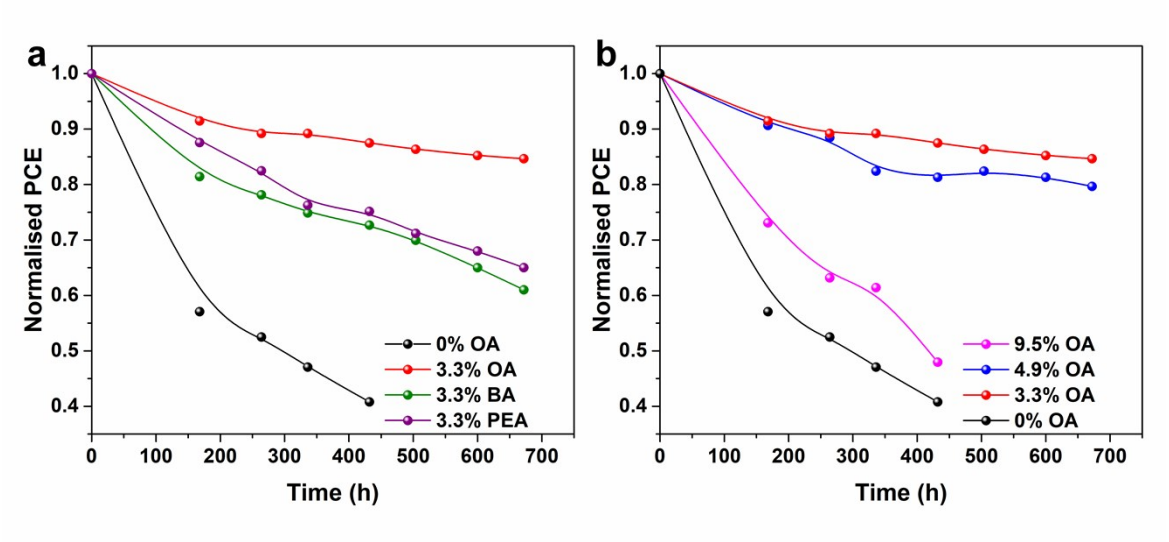

Fig. S10 The variation in normalized PCEs of the devices with (a) 0% OA, 3.3% OA, BA, and PEA contents, and with (b) different OA contents. All thermal stability testing were performed in an oven in ambient atmosphere at 85 °C without any encapsulation.

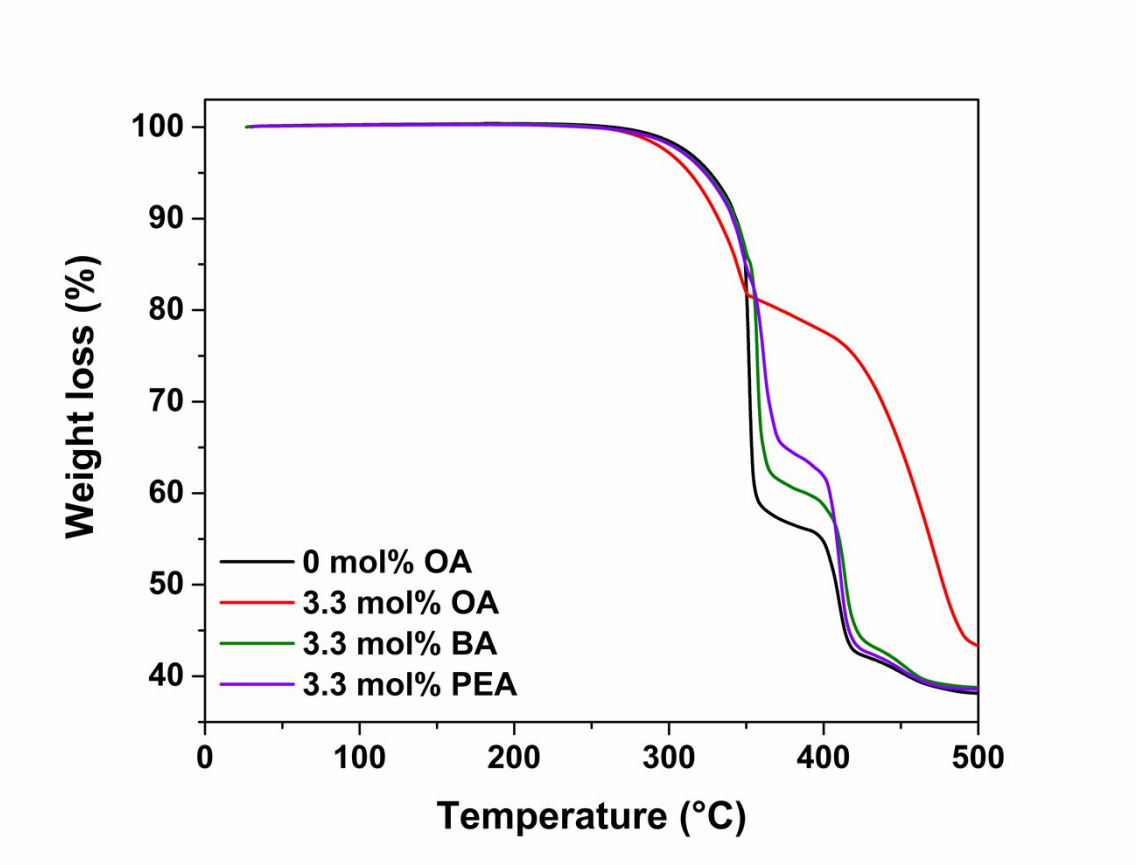

Fig. S11 Thermogravimetric analysis (TGA) curves of the perovskites with unmodified, 3.3% OA, BA, and PEA contents. The analysis was performed from 25 °C to 500 °C with a ramping rate of 10 °C min^{-1} in air.

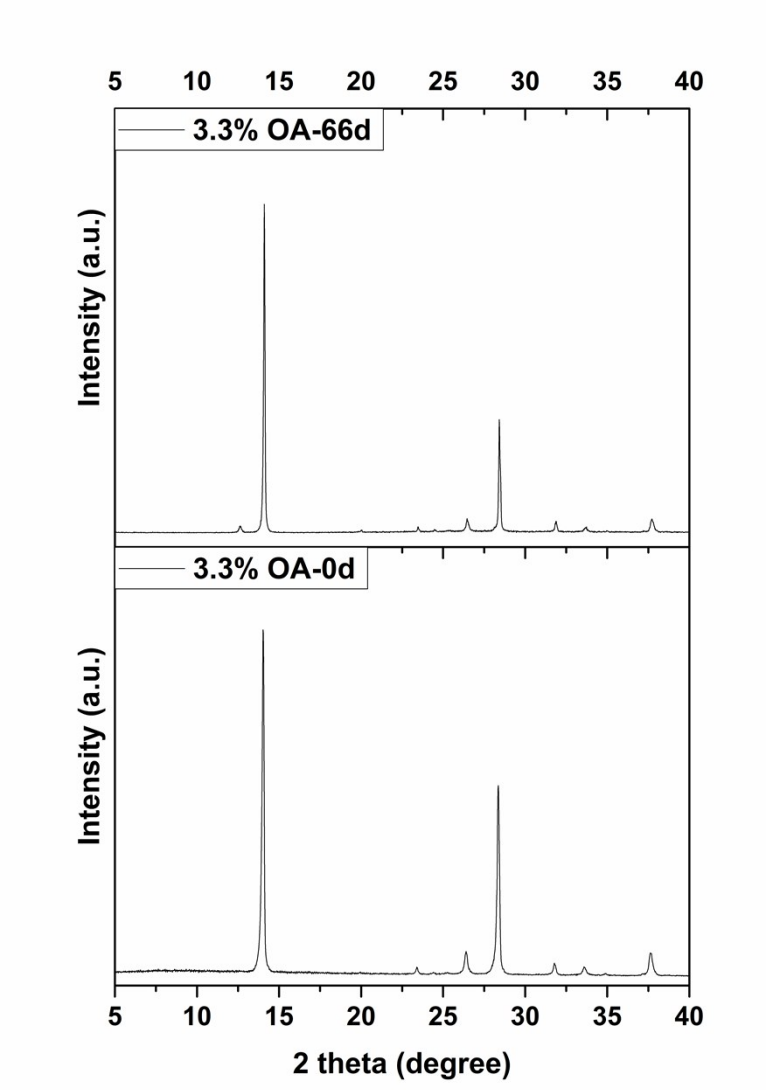

Fig. S12 XRD patterns of 3.3% OA-modified $MAPbI_3$ (a) prior to and (b) following stability test at room temperature and under 25 % relative humidity for 66 days.

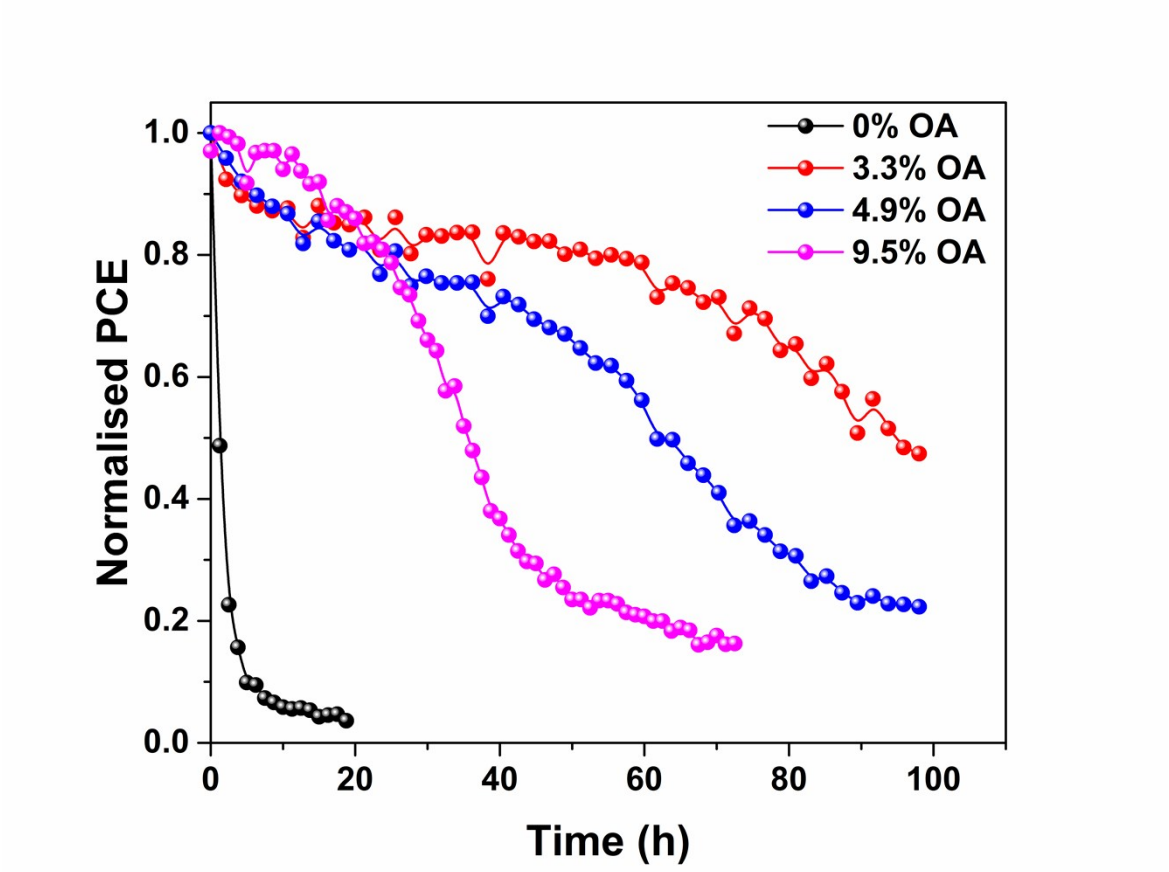

Fig. S13 Photostability of OA-modified perovskite solar cells ranging from 0 to 9.5% OA contents without any encapsulation under constant AM 1.5G illumination without a UV blocking filter in N_2 atmosphere at room temperature.

Table S1 Charge carrier recombination lifetimes of OA mixed perovskite films with 0 to 9.5% OA contents. The values are calculated from Fig. 1c.

OA content (%)	τ_1 (ns)	τ_2 (ns)	A_1	A_2	τ_{ave} (ns)
0	1.93	38.0	0.23	0.77	37.5
3.3	8.60	157.5	0.05	0.95	157.1
4.9	7.95	123.3	0.10	0.90	122.5
9.5	4.46	71.0	0.18	0.82	70.1